Environmental Science
Water Research & Technology

ROYAL SOCIETY OF CHEMISTRY

PAPER

View Article Online
View Journal | View Issue

Check for updates

Cite this: *Environ. Sci.: Water Res. Technol.*, 2024, **10**, 2075

Uranium rejection with nanofiltration membranes and the influence of environmentally relevant mono- and divalent cations at various pH†

Christopher B. Yazzie,[a] Catalina Elias[b] and Vasiliki Karanikola *[a]

Nanofiltration (NF) can be used as a low-energy pressure-driven membrane treatment process with potential applications in mitigating uranium contamination from groundwater. Uranium can interact with groundwater minerals which can influence NF uranium rejection. This study used two commercially available membranes (NF90 and NF270) to remove uranyl complexes in the presence of environmentally relevant cations (Na^+, Mg^{2+}, and Ca^{2+}). The analysis includes extensive membrane characterization, calculating NF treatment performance, investigating uranium adsorption to the functionalized polyamide top layer of the membrane, and determining membrane selectivity. Under batch experiments, using environmentally relevant ion concentrations, we measured uranium rejection rates for the NF90 between 58–99% and NF270 between 4–98%. The mechanisms of low uranium rejection are not only explained by steric hindrance but also by the reduction of the Donnan exclusion mechanism, which originates from the decrease in membrane charge density caused by the addition of mono- and divalent ions. Additionally, exclusion mechanisms were observed to be directly influenced by solution pH, which governs the variation in uranyl complexation type and membrane charge. Calcium has a complexation affinity to uranium with broad implications in uranyl-complex molecular weight, valance, and molecular shape, all of which can influence water treatment efficiency. Lastly, both membranes were evaluated based on their membrane selectivity, the ratio of cation fluxes to uranium(VI) ion flux. Ideal membrane selectivity occurred at pH 7. Na^+ to uranium(VI) ion ratio was 190 for NF90 and 100 for NF270. The results of this study advance the understanding of using NF membranes for groundwater uranium removal.

Received 21st April 2024,
Accepted 25th June 2024

DOI: 10.1039/d4ew00324a

rsc.li/es-water

Open Access Article. Published on 25 Fõndo 2024. Downloaded on 13/2/2026 19:33:08.
This article is licensed under a Creative Commons Attribution 3.0 Unported Licence.

Water impact

Our study investigates nanofiltration as a possible process to treat uranium-contaminated groundwater. We provide information on how uranium removal is affected by major ions, which is critical for process efficacy when treating groundwater with variable water chemistries. Results from this study will help advance sustainable, safe drinking water.

Introduction

Access to clean water is an inherent human right. To support this right the United Nations (UN) has adopted the Sustainable Development Goal 6: ensuring access to clean water and sanitation for all.[1] It is estimated that up to a third of the world's population lacks access to safe (monitored) water.[2] Non monitored (or regulated) water can harbor contaminations, impact human health and cause ecosystem degradation. In arid environments reliance on groundwater is vital yet water quality monitoring is often overlooked due to economic and geographic inaccessibility which results in exposing populations to hazardous contaminations.[3] As climate change becomes increasingly more pronounced, freshwater management redirects readily available groundwater and freshwater sources away from rural areas. This is especially true, in mining regions around the world, where groundwater and surface waters have been affected by mining a plethora of metals; an example is the environmental dispersion of uranium, which has contaminated previously clean water aquifers, introducing pathways for human exposure to heavy metals.[4,5]

Uranium, a heavy metal, is abundant in the Earth's crust and oceans.[6] It is geologically located in ancient sedimentary basins or igneous formations, reducing overtime to

[a] *Chemical and Environmental Engineering Department, University of Arizona, Tucson, Arizona, 85721, USA. E-mail: vkaranik@arizona.edu; Tel: +1 (520) 621 5881*
[b] *Biosystems Engineering Department, University of Arizona, Tucson, Arizona, 85721, USA*

† Electronic supplementary information (ESI) available. See DOI: https://doi.org/10.1039/d4ew00324a

Open Access Article. Published on 25 Föndo 2024. Downloaded on 13/2/2026 19:33:08.
This article is licensed under a Creative Commons Attribution 3.0 Unported Licence.

uranium(IV) and integrating with local minerals. Mining processes dislodge uranium minerals, while residual materials oxidize to uranium(VI), which complexes with various ligands and can transport aqueously in the environment.[7] Human exposure occurs primarily through water but also through air. Once inside the human body, uranium is metabolically inert, accumulating in the liver, kidneys, and bones.[8,9] Uranium is also a radioactive element that releases alpha and beta particles, which can damage genetic material. The United States Environmental Protection Agency (USEPA) has set the maximum contaminant level (MCL) for uranium at 30 μg L^{-1}, enforceable only for water systems serving more than 30 people; comparatively, the European Union (EU) and UN have stricter guidelines at 10 μg L^{-1}. Regions in the Southwestern United States, Eastern Germany, Central China, and Western Australia all have groundwater sources exceeding 100 μg L^{-1} of uranium; therefore, a significant reduction of its concentration is necessary before human use to meet water quality standards and human rights goals.[7,10–12]

Because of the toxicity of uranium, to remove it from water, the USEPA has established several best available technologies (BAT) to mitigate the contamination issues.[13] Ion exchange (IX) uses resins to exchange uranium with other ions and thus trapping uranium in the resin, but its regeneration requires strong chemicals, and the process produces secondary waste. Lime softening utilizes calcium hydroxide, another strong chemical, to raise the pH which allows for uranium to precipitate and remove it through sedimentation and filtration. Enhanced coagulation/filtration removes uranium by adding coagulants to water, which causes uranium and particles to clump together; this process also requires strong chemicals and creates a secondary waste stream. Although several technologies exist to purify groundwater, many are not economically feasible for rural populations, or their operational and maintenance requirements exceed rural technical capabilities.[14] Nanofiltration (NF) membrane is pressure-driven processes that selectively remove divalent over monovalent ions and can offer affordable, easy-to-operate, and maintain solutions that can effectively remove many water contaminants.[15]

Several studies have examined both organic and inorganic NF membranes for water treatment, including industrial wastewater, groundwater treatment, the removal of organic matter from surface water, and resource recovery from seawater.[15–18] There is an abundance of literature that focuses on membrane fouling, surface modification for improved performance, and removal efficiencies which all provide operational strategies and information on ion rejection mechanisms.[19–21] Some bench-scale studies report high rejection rates of uranium however, most of the experiments were conducted at environmentally unrealistic feed stream concentrations (>1000 μg L^{-1}).[22–25] Furthermore, one study showed that uranium ions can adsorb in the membrane support materials, which can pose disposal challenges for spent membranes.[26] It should be highlighted here that NF performance relies both on size and Donnan exclusion mechanisms and both contribute to the selective nature of the membrane between monovalent and larger ions.[27–29] This is important as groundwater ion speciation studies showed there is a wide variability of different size, shape and charge ions that can affect uranium rejection.[11,30,31] Previous studies have shown the importance of pH variation in solution and how it affects uranyl complexation affinities to certain minerals.[32,33] Aqueous uranyl complexes vary in size and charge depending on pH and mineral availability, which in turn significantly alters membrane surface charge interactions.[11,30] For several of the BAT methods of uranium removal, the presence of groundwater minerals such as calcium and the size and charge of uranyl complexes reduces changes their efficiencies. To our knowledge, no studies have explored the influence of environmentally relevant groundwater cation minerals at different ionic concentrations and pH on NF uranium rejection.

The objective of this study is to evaluate NF membrane uranium rejection and selectivity over relevant groundwater cations (Na^+, Mg^+, and Ca^{2+}) across various pHs. We integrated batch bench-scale experiments with inductively coupled plasma mass spectrometry, ion chromatography, water chemistry modeling, and membrane characterization tools to examine the performance of uranium rejection from two commercially available NF membranes (NF90 and NF270). Operation conditions were chosen to mimic smaller water systems without surplus energy sources that would operate at low pressures pump (75 pounds per square inch (psi)), and using uranium concentrations typical to groundwater (150 μg L^{-1}) in the Southwestern United States. The novelty of this study is the differentiation of the effects of co-occurring cations on uranium exclusion and showing the effects on uranium rejection performance, membrane selectivity, and adsorption effects using environmentally relevant conditions. Results of this study show the physiochemical effects of solution with monovalent and divalent ions on uranium rejection, which ultimately can be relevant for water treatment technologies using NF processes in rural communities around the world.

Material and methods

Materials

The rejection of uranium was examined using a feed solution surrogate containing 150 μg L^{-1} uranium, added as uranyl nitrate ($UO_2(NO_3)_2{\cdot}6H_2O$, Sigma-Aldrich), while varying concentrations between 1 mg L^{-1} and 5 mg L^{-1} of sodium chloride (NaCl, Spectrum Chemical), magnesium chloride ($MgCl_2$, Spectrum Chemical), and calcium sulfate ($CaSO_4$, Sigma-Aldrich). Hydrochloric acid (HCl 1 M, Sigma-Aldrich) and sodium hydroxide (NaOH 1 M, Sigma-Aldrich) were utilized for pH adjustment. All solutions were mixed with deionized water (DI) (Milli-Q water, Millipore-Merck) ultra-pure water, and trace grade 2% nitric acid (67% HNO_3,

 This journal is © The Royal Society of Chemistry 2024

Open Access Article. Published on 25 Föndo 2024. Downloaded on 13/2/2026 19:33:08.
This article is licensed under a Creative Commons Attribution 3.0 Unported Licence.

Sigma-Aldrich) was used as a preserving agent for ion coupled plasma mass spectrometry (ICP-MS) analysis.

Uranium water chemistry analysis

Uranium speciation was computed with the water chemistry software Visual Minteq 3.1 (Stockton, Sweden), updated in February 2019.[34] Multiple separate sweep test computations were conducted across pH ranges 4–10 using experimental conditions in the NF bench scale experiments. Uranium concentration was set to 150 μg L^{-1}, temperature was designated to 25 °C, and CO_2 pressure was assumed as atmospheric pressure (0.038 mbar). Separate computations were conducted with the individual addition of 1 and 5 mg L^{-1} NaCl, 1 mg L^{-1} $CaSO_4$, and 1 mg L^{-1} $MgCl_2$.

Membrane preparation

Two commercial NF membranes with different aromatic polyamide structures were used: NF270 (Dow FilmTec), and NF90 (Dow FilmTec). Sheet dimensions of the working area of the membrane were 95 mm wide and 145.5 mm long and were supported by a feed channel spacer and permeate channel carrier spacer. A feed flowrate of 30 liters per hour (LPH) was used during experiments which translated to a feed cross-flow velocity at 0.044 m s^{-1}. Prior and between experiments, membranes were stored in deionized water that was periodically changed. Prior to experiments, membrane compaction included a 24-hour soak in DI, and operation in the membrane cell with DI at 75 psi for 24 hours. Experiments were operated at 75 psi, and when a pH change occurred, one hour of operation was allowed for the system to come to a steady state before sampling.

Cross flow device setup and procedures

A HydraCell metering pump powered by a 1/3 HP WattSaver motor (Leeson, USA) with a Speedmaster adjustable speed AC motor control (Leeson, USA) was used for the NF system. Operational pressure was dictated by the pump power setting (pump speed) and the valve restricting crossflow, located just beyond the pressure gauge in the recirculation line (Fig. S1†). The pump produced flow proportional to the rpm setting and independent of the pressure required. The pump speed was set using a control box mounted by the device and was set to a constant 25 Hz. The flow-restricting valve was manually set to 75 psi and had to be adjusted throughout the experiment. Feed water pressure was kept between 72 and 78 psi during experiments. The feed flow rate was constant at 30 LPH, and the permeate, that was not collected as the sample, was also returned to the feed tank along with the brine (retentate stream).

Water sampling analysis

U^{6+}, Mg^{2+}, Na^{+}, and Ca^{2+} concentrations from feed and permeate were quantified with inductively coupled plasma-mass spectrometry (ICP-MS, Elan DRC-II), using EPA Method 6020B (US. EPA 2014). Ca^{2+} determination was aided using strontium to determine known interference. Standards were prepared from certified solutions (Fisher Scientific, Pittsburg, PA). NO_3^{2-}, SO_4^{2-}, and Cl^{-} from feed and permeate were quantified by ion chromatography (Thermo Scientific IC Dionex 3001), using EPA Method 300.1 (US. EPA, 1999), and standards were prepared from certified solutions (Fisher Scientific, Pittsburg, PA).

Streaming zeta potential measurements

Streaming zeta potential measurements were performed (Anton-Parr SurPASS 3, Austria) using a flat sheet gap analyzer attachment to determine the difference in surface electrical charge between new and used membranes. A 1 mM KCl buffer was used in all experiments, and 1 mM HCl and 1 mM NaOH solutions were used to alter the pH. pH was initially brought to approximately 10, and zeta potential measurements were taken 4 times, then presented as an average. pH was then repeatedly lowered by approximately 1 pH unit and the zeta potential was again measured. This process continued to approximately pH 4. pH iso-electric points (IEP) were measured separately by using 0.1 M HCl until the zeta potential measurements gave positive readings, which then allowed interpolation to find the IEP. All zeta potential experiments were carried out at room temperature (approximately 22 °C).

Uranium adsorption to the polyamide layer of the membrane

Experiments were conducted to evaluate the uranium adsorption capacity of the polyamide layer in the NF90 and NF270 membranes. Our focus was on the adsorption properties of the polyamide top layer; thus, it was isolated from the membrane's lower support layers. Membrane coupons were cut into sizes approximately 20 × 10 mm and were precisely measured with a caliper measuring device. Separate batch experiments were performed, each containing 150 μg L^{-1} of uranium in one of these solutions: 1 g L^{-1} NaCl, 1 g L^{-1} MgCl, or 1 g L^{-1} $CaSO_4$. A membrane coupon and 10 mL of the solution were placed into a 15 mL tube for each experiment. Each solution was prepared at two pH levels: pH 3.8, corresponding to the approximate isoelectric point of the membrane, and a neutral pH of 7. This assembly was agitated on a shaker plate for 48 hours to reach adsorption equilibrium. Each variable change was done in triplicates to ensure reliable results. Post-experiment, inductively coupled plasma mass spectrometry (ICP-MS) analysis was used to quantify the concentrations in the solution. A mass balance approach was used to ascertain the amount of uranium adsorbed onto each membrane coupon.

Calculations

Concentration polarization (CP) was calculated using methods described in previous literature,[35–37] and the CP modulus is expressed as the following equation:

Open Access Article. Published on 25 Föndo 2024. Downloaded on 13/2/2026 19:33:08.
This article is licensed under a Creative Commons Attribution 3.0 Unported Licence.

$$\mathrm{CP} = \frac{C_{\mathrm{membrane}} - C_{\mathrm{permeate}}}{C_{\mathrm{feed}} - C_{\mathrm{permeate}}} = \exp\left(\frac{J_w}{k}\right) \quad (1)$$

where k (m s^{-1}) (eqn (S2)†) is the mass transfer coefficient, which is determined using the Sherwood (eqn (S1)†), Reynolds, and Schmidt equations, a detailed description of additional equations used to solve the CP is found in the ESI.†

Real rejection was calculated employing the following equation:

$$R_r = 1 - \frac{C_{\mathrm{permeate}}}{C_{\mathrm{membrane}}} \quad (2)$$

where C_{membrane} is the solute feed concentration at the membrane wall and C_{feed} is the solute feed concentration in bulk solution.

Membrane selectivity (MS) is the ratio of concentration transmissivity and is given by the following equation.

$$\mathrm{MS} = \frac{\frac{C_p^i}{C_f^i}}{\frac{C_p^{U(VI)}}{C_f^{U(VI)}}} \quad (3)$$

where C_p^i represents solute i concentration in the permeate stream, C_f^i is the concentration of solute i in the feed stream, $C_p^{U(VI)}$ is the concentration of uranium in the permeate stream, and $C_f^{U(VI)}$ is the concentration of uranium in the feed stream. The concentrations in this equation are after CP effect has been added.

Adsorption of uranium onto the membrane surface was calculated using the following mass balance equation.

$$m_a = (C_i - C_e) \times V \quad (4)$$

where m_a is the mass absorbed to the membrane, C_i is the initial concentration of uranium, C_e is the concentration of uranium at equilibrium and V is the volume of solution used in the experiment.

Results

Membrane characterization

NF90 and NF270 membrane distribution of electrically charged ions near the surface of a membrane were characterized. The membrane charge is referred to as zeta potential and is the electric potential density at the "shear plane" boundary layer, which divides nonmoving and movable layers of charges very close to the membrane surface. Interaction between the solid surface of the membrane and aqueous solutes can depend on either repulsion or attraction phenomena.[38] For membrane water treatment processes, the repulsion strength of the membrane surface potential with similarly charged ions within the bulk solution gives rise to the rejection of ions in the feed stream, which is known as the Donnan rejection mechanism.

NF90 and NF270 membrane charge characteristics were measured by streaming zeta potential and presented as a function of pH (Fig. 1). The measured streaming zeta potential is negative for both membranes within the pH range of 4–8 for all experimental solutions tested. The addition of salts ($UO_2(NO_3)_2{\cdot}6H_2O$, NaCl, $MgCl_2$, and $CaSO_4$) significantly reduced the surface negativity of both NF90 and NF270 zeta potentials with the divalent salts ($MgCl_2$ and $CaSO_4$), showing a more significant reduction in the streaming zeta potential. The NF270 (Fig. 1B) showed a higher negative zeta potential than NF90 (Fig. 1A), which can be explained by the differences in functional groups of the polyamide (PA) layer of each membrane. In separate experiments, the IEP was found to be ~4.0 and ~3.7 for the NF90 and NF270, respectively (Table 1). The IEP is the pH where the charge of the membrane is neutral and is important for operational and design considerations.

Both membranes' initial negative surface charge can be attributed to the density of PA functional groups on the membrane's surface, which is a by-product of the interfacial polymerization manufacturing process. The PA layer consisting of cross-linked aromatic groups such as carboxylic (COO–) and amines (NH_2–) is fully aromatic for the NF90 and semi-aromatic for the NF270. The density of the PA cross-linked layer also determines the membrane pore radius, thus theoretically increasing the NF90 solute rejection by the steric (size) mechanism.[40] A collection of membrane characteristics is found in Table 1.

The decreased negativity of streaming zeta potential by the addition of high concentrations of ions could result from the electrostatic adsorption between cation solutes and

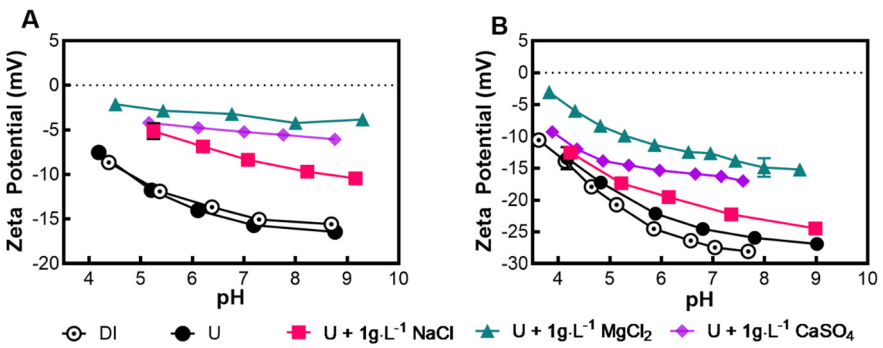

Fig. 1 Streaming zeta potential (mV) scans over pH ranges for A) NF90 and B) NF270 membranes. Additional tests included the addition of ions: $UO_2(NO_3)_2{\cdot}6H_2O$, NaCl, $MgCl_2$, and $CaSO_4$.

 This journal is © The Royal Society of Chemistry 2024

Table 1 Membrane characteristics

Membrane	PA type	Iso electric point (pH)	Pore radius (nm)	Water flux (LMH)
NF90	Fully-aromatic	4.0	0.34	56.5
NF270	Piperazine-based semi-aromatic	3.7	0.42	88.5

Notes: pore radius information was obtained from Nghiem *et al.*[39] Water flux was measured using deionized water at 22 °C and operating the nanofiltration system at a pressure of 75 psi. Additional information on results is included in the ESI,† Fig. S8.

Open Access Article. Published on 25 Fõndo 2024. Downloaded on 13/2/2026 19:33:08.
This article is licensed under a Creative Commons Attribution 3.0 Unported Licence.

negatively charged membrane functional groups; thus, divalent ions would have a more significant adverse effect on the neutralization of the membrane charge. The electric double layer would also shrink due to increased charged solutes near the membrane surface. Collectively, these effects can give ions in the bulk solution a greater chance of being transported through the membranes. Since the measured zeta potential is negative throughout the experimental pH range, the valence of uranyl complexes will significantly impact whether the molecule is attracted, repelled, or neutral relevant to the membrane, which is an important factor in the Donnan exclusion mechanism of uranium complexes.

Water chemistry modeling

To understand the interactions between uranium, various aqueous minerals and gases, we used the water chemistry analysis modeling software Visual Minteq 3.1 2019 (Stockholm, Sweden). In natural waters, uranium can complex with various dissolved inorganic minerals originating from local geology.[11] The modeling input concentrations were chosen based on experimental conditions that reflect natural groundwater sources where uranium is an issue of concern.[4,10] Overall, results show uranium's aqueous chemical behavior depends on solution pH and the availability of various solute minerals (Fig. 2).

Fig. 2A shows the water chemistry modeling results of adding $UO_2(NO_3)_2{\cdot}6H_2O$ in water solution (U(VI) 150 μg L^{-1}) in contact with atmospheric carbon dioxide (0.38×10^{-3} atm CO_2) at various pHs. In the system solution of Fig. 2A, the four main uranium complexes in the order of increasing pH are: UO_2^{2+}, UO_2OH^+, $(UO_2)_2CO_3(OH)_3^-$, and $(UO_2)_2CO_3^{4-}$. At pH 6, carbon dioxide enters the system, increasing the uranyl complex's molecular weight and the valence of uranyl-complex molecules. The addition of 1 g L^{-1} NaCl (Fig. S2†) and 1 g L^{-1} $MgCl_2$ (Fig. S3†) into the model did not influence variation in uranium complexation compared to Fig. 2A. In contrast, the addition of 1 g L^{-1} $CaSO_4$ (Fig. 2B) promotes calcium and sulfate-containing uranyl complexes. The four main uranium complexes across the pH range 4–10 in the $CaSO_4$ solution are UO_2SO_4, $(UO_2)_2CO_3(OH)_3^-$, $Ca_2UO_2(CO_3)_3$, and $CaUO_2(CO_3)_3^{2-}$. The preference of uranyl to complex with calcium rather than other cations such as sodium and magnesium cannot be easily explained, but studies have identified physiochemical characteristics such as the size and shape of calcium and uranium influencing the affinity of the two ions.[41]

Major uranyl complexes found in this study are described in Table 2. The speciation modeling shows carbonate complexes with uranium at pH greater than 6 due to the carbon dioxide contribution from the atmosphere entering the system and reverting to carbonate due to the equilibrium shift of carbonic acid. Similar influences with carbonate complexes have been observed in both theoretical kinetic studies and laboratory studies.[42–44] Typically, uranyl complexes have their lowest molecular weight at the low pH's (4–5.5), and as pH increases (7–8.5), the molecular weight increases to the largest observed uranyl complexes, and

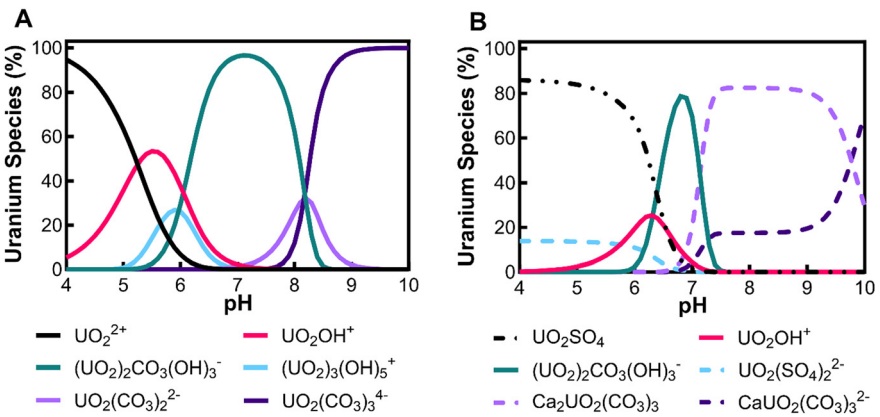

Fig. 2 Uranium speciation modeling using Visual Minteq 3.1 2019 (Stockholm, Sweden). Both computations simulated an open system with carbonate at atmospheric concentrations (0.38×10^{-3} atm CO_2). A) Open system uranyl speciation with uranium concentration of 150 μg L^{-1}, B) open system uranyl speciation with uranium concentration of 150 μg L^{-1} and $CaSO_4$ 1 g L^{-1}.

Open Access Article. Published on 25 Föndo 2024. Downloaded on 13/2/2026 19:33:08.
This article is licensed under a Creative Commons Attribution 3.0 Unported Licence.

Table 2 Summary of major uranyl water chemistry characteristics across a range of pH

pH	Major uranium complex	Molecular weight (g mol^{-1})	Complex shape	Source of shape
4	UO_2^{2+}	270.03	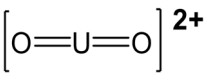	45
	UO_2SO_4	366.09	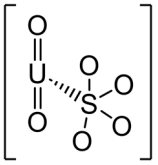	46
5.5	UO_2^{2+}	270.03	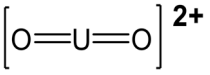	45
	UO_2OH^+	287.04	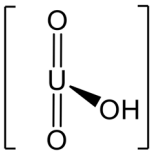	—
7	$(UO_2)_2CO_3(OH)_3^-$	651.094	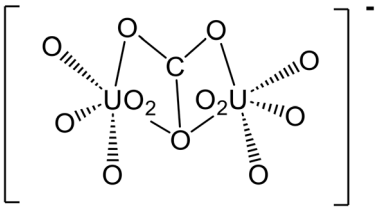	47
	$Ca_2UO_2(CO_3)_3$	530.22	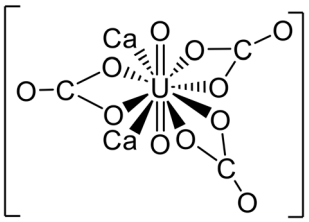	48
8.5	$Ca_2UO_2(CO_3)_3$	530.22	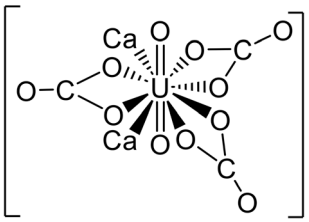	48
	$(UO_2)_2CO_3^{4-}$	600.07	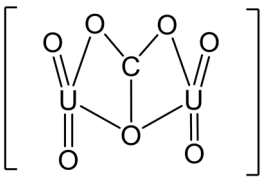	47
10	$(UO_2)_2CO_3^{4-}$	600.07	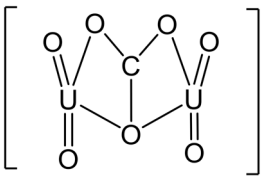	47
	$CaUO_2(CO_3)_3^{2-}$	490.14	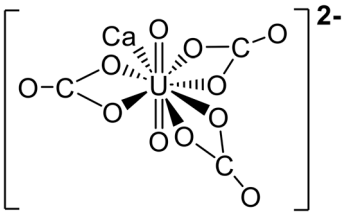	48

This journal is © The Royal Society of Chemistry 2024

Open Access Article. Published on 25 Föndo 2024. Downloaded on 13/2/2026 19:33:08.
This article is licensed under a Creative Commons Attribution 3.0 Unported Licence.

finally, the molecular weight decreases slightly at pH 10 as shown in Table 2. Also, the valence charge of the uranyl-complexes changes with pH and shows a tendency to have negative attributes at a low pH, a neutral valence charge at a neutral pH, and a positive at a higher pH. The valence charge association with pH follows water hydrolysis with excess protons at low pH and excess hydroxide molecules at higher pH.

In literature, uranyl–calcium complexes are the most common aqueous uranyl complexes found in nature.[43,49] At low pH, the neutrally charged uranyl sulfate complexes can be found where uranium mining has occurred due to the use of sulfuric acid in ore processing.[11] Chemistry and minerals present in water are specific to regional geology and anthropogenic activities close to groundwater aquifer sources. For example, in the Navajo Nation, USA, uranium mill tailing processing sites have reported high levels of groundwater sulfate contamination.[50,51] The uranium uptake in humans is concentrated in bones and teeth, further identifying the importance of removing uranyl–calcium complexes.[9] The tendency for uranyl to complex with calcium is known to limit the performance of adsorption mechanism techniques in removing uranium from aqueous solutions; however, with membrane processes, the increase in molecular weight and valence charges can improve water treatment efficiency.[33,52]

Nanofiltration uranium rejection performance

Given the relatively high water flux of nanofiltration (NF) membranes compared to reverse osmosis membranes, the concentration polarization (CP) (as defined in eqn (1)) was calculated for each experimental condition containing uranium. The CP results are presented in Tables S1 and S2,† revealing that NF270 is more prone to CP than NF90. This is consistent with the established principle that CP intensifies with increased membrane water flux due to the increased concentration of rejected ions against the membrane's surface. The relatively slow ion diffusion rate back into the bulk solution results in operationally high concentrations against the membrane, resulting in higher solute flux and a more significant opportunity for adsorption. Factoring in CP, uranium concentrations at the feed-side membrane surface can rise by 2–15% for NF90 and 9–24% for NF270 compared to the bulk solution concentration, making CP an essential operational parameter to consider.

Accounting for CP, the real uranium rejection (eqn (2)) performance across a pH range of 4–10 for NF90 and NF270 membranes is depicted in Fig. 3. The rejection of uranium is dependent on pH, mainly due to the variation of uranyl complexes occurring throughout the experimental pH range. The change in pH and the addition of cations will alter the uranyl molecule characteristics, such as valence charge, size, and shape, with pH, as we see in Table 2. The NF90 membrane consistently rejected over 98% of uranium in feed solutions at pH levels from 5.5 to 8.5 and maintained rejections above 90% at pH 10. For NF270, uranium rejections varied between 80–98% within the pH range of 5.5–10. Previous studies show that NF90 has a tighter PA layer than NF270, which explains the higher rejection in NF90 over NF270.[53] Both membranes showed their lowest uranium rejection rates at pH 4, with NF90 having rejection rates between 58–83% and NF270 between 4–78%. The reduced rejection at pH 4 coincided with the highest uranium flux for both NF90 and NF270 membranes, as calculated in eqn (S3) and illustrated in Fig. S3 and S4.†

The observed decrease in uranium rejection across different experimental conditions can be attributed to Donnan and steric exclusion mechanisms. The introduction of mono- and divalent ions increases the ionic strength of the solution, therefore increasing osmotic pressure and reducing the membrane's streaming zeta potential by compressing the electric double layer. This compression results in decreased membrane charge density and thickness, potentially allowing uranyl complexes to permeate the membrane, irrespective of their charge. NF270 is known from

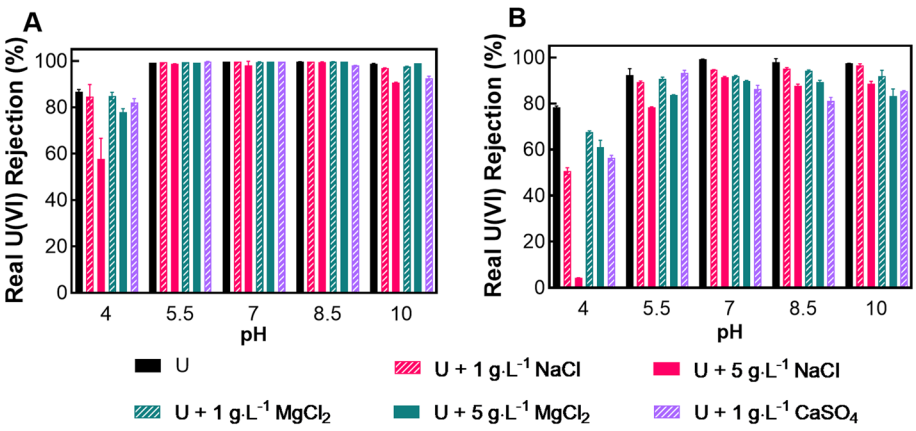

Fig. 3 Comparative uranium rejection by A) NF90 and B) NF270 membranes at different pH levels and ionic conditions. All solutions in these tests contained 150 μg L^{-1} of uranium (added as $UO_2(NO_3)_2{\cdot}6H_2O$) and operated at 22 °C and 75 psi. Error bars are included to describe the standard error of the mean.

Open Access Article. Published on 25 Föndo 2024. Downloaded on 13/2/2026 19:33:08.
This article is licensed under a Creative Commons Attribution 3.0 Unported Licence.

previous studies to have large nominal pores and therefore ion rejection heavily relies on Donnan exclusion mechanisms. Fig. 3B shows a decrease in uranium rejection for the NaCl and $MgCl_2$ solutions. In literature, we see the correlation between a reduction in membrane charge with these salts and a reduction in ion rejection.[53] The NF90 (Fig. 3A) showed a similar reduction of ion rejection at low pH (4.0) and high pH.[10] The lowest uranium rejection observed in this study occurred with the NF270, operating at pH 4, and with 5 g L^{-1} NaCl solution. It has been noted in literature that large concentrations of NaCl cause an irreversible pore swelling effect, thus increasing the membrane pore size possibly in both membranes.[54] Analysis of zeta potential measurements (Fig. 1) also revealed that divalent ions exert a more pronounced effect on streaming zeta potential reduction than monovalent ions. Instances like those shown in Fig. 1B (NaCl and $MgCl_2$ at pH 7) highlight divalent ion solutions with lower uranium rejections than those with monovalent ions, suggesting divalent ions decrease the Donnan exclusion mechanism due to reduced membrane charge density. Further, at pH 4, the least negative streaming zeta potential and the lowest uranium rejection were observed, indicating the need to maintain and adjust pH to the range of 5.5–8.5 for optimal uranium rejection performance.

The valence of uranyl complexes changes with experimental conditions, and $CaSO_4$ was selected to illustrate how uranyl complex characteristics differ in size and valence. At low pH levels in calcium-free solutions, the dominant species is UO_2^{2+}, with a valence charge of 2+. However, in the presence of $CaSO_4$, a neutrally charged UO_2SO_4 is most common until approximately pH 6 (Fig. 2B). Regarding rejection, UO_2SO_4 has a greater rate than UO_2^{2+}, suggesting that molecular weight is a more critical factor for uranium rejection than charge at low pH. In the $CaSO_4$ solutions, calcium–uranyl–carbonate complexes are prevalent at neutral to high pH, with $Ca_2UO_2(CO_3)_3$ having a neutral charge and $CaUO_2(CO_3)_3^{2-}$ having a 2− charge. Again, we see the molecule with the larger molecular weight $Ca_2UO_2(CO_3)_3$, found at pH 8.5, having a greater rejection for the NF270 (Fig. 2B).

In neutral to high pH ranges, uranium complexes tend to have larger molecular weights, and consequently uranium rejection, for both membranes, increases. This pattern implies that steric exclusion mechanisms significantly influence uranium transport through both membranes. For example, the uranyl–calcium complexes have lower molecular weight and valence magnitude than their uranyl–carbonate counterparts in solutions without calcium. We observed that the calcium uranyl–carbonate complexes have a noticeably lower rejection for an NF270 membrane compared to uranyl–carbonate complexes that are prevalent in the solution not containing calcium. Lastly, our analysis did not include the shape and radius of uranyl complexes in their association with rejection. Still, it is possible that $(UO_2)_2CO_3(OH)_3^-$ and $(UO_2)_2CO_3^{4-}$ are larger than their calcium–uranyl–carbonate counterparts due to central carbonate molecules connected to two uranyl molecules (as seen in Table 2), thus rendering a molecule with a larger radius.

Uranium adsorption to nanofiltration membranes

Our study examined uranium adsorption onto the surface of NF membranes. While previous research has investigated uranium adsorption, mainly focusing on its incorporation within the polysulfone support layer, findings regarding surface adsorption remained inconclusive.[26] Consequently, our research specifically addressed the polyamide (PA) surface of the membrane, an aspect unexplored. This investigation required the isolation therefore, detachment of the PA layer from its supporting layers before experimentation. Our experiments evaluated various membrane types, two pH levels, and different cations to determine uranium adsorption capacity.

We explored the interactions between solutes and membranes at the membranes' IEP and neutral pH levels. The analysis of the NF90 and NF270 membranes' adsorptive behavior toward uranium(VI) (Fig. 4) shown a pH dependency. At pH 4, where the membrane's zeta potential is approximately zero, both membranes exhibited adsorption capacity ranging from 0.55 to 1.55 mg U(VI) per m^2, across all solution types. At these conditions, uranyl is formed (UO_2^{2+}) in the presence of NaCl and $MgCl_2$. With a $CaSO_4$ solution, the uranyl complex becomes UO_2SO_4, which possesses a neutral valence. This indicates that electrostatic interactions are not the primary mechanisms for adsorption at low pH. When neutral pH 7 was tested, the membranes exhibit a negative zeta potential across all tested solutions, implying the deprotonation of functional sites on the membrane. Under these conditions, adsorption rates for both membranes increased to approximately 4.25 mg U(VI) per m^2, except in the presence of $MgCl_2$, where it was slightly lower (3 mg U(VI) per m^2 for NF90 and 3.8 mg U(VI) per m^2 for

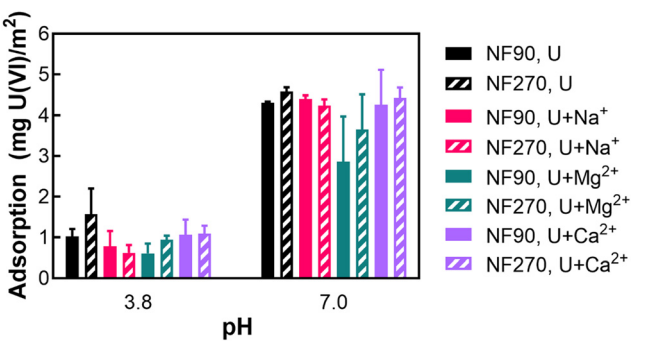

Fig. 4 Comparison of uranium(VI) adsorption by NF90 and NF270 at membrane iso-electric point (~3.8) *versus* neutral pH (~7.0). All solutions in these tests contained 150 μg L^{-1} of uranium (added as $UO_2(NO_3)_2{\cdot}6H_2O$) and were conducted at 22 °C. pH adjustments were made using 2% HNO_3 and 1 mM NaOH. Error bars are included to describe the standard error of the mean.

This journal is © The Royal Society of Chemistry 2024

Open Access Article. Published on 25 Föndo 2024. Downloaded on 13/2/2026 19:33:08.
This article is licensed under a Creative Commons Attribution 3.0 Unported Licence.

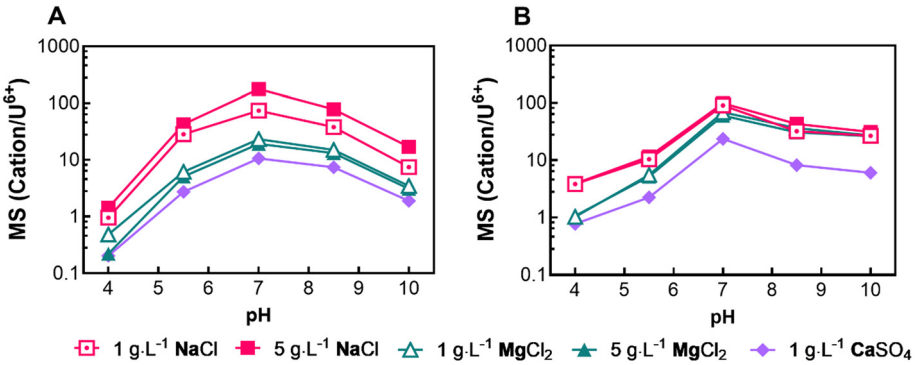

Fig. 5 Membrane selectivity for A) NF90 and B) NF270 based on the transmission ratio of cations to uranium. All solutions in these tests contained 150 μg L^{-1} of uranium (added as $UO_2(NO_3)_2{\cdot}6H_2O$) and were conducted at 22 °C. pH adjustments were made using 2% HNO_3 and 1 mM NaOH.

NF270). Uranyl forms the complexation $(UO_2)_2CO_3(OH)_3^-$ in NaCl and $MgCl_2$ solutions at neutral pH. In the presence of $CaSO_4$, the complex is $Ca_2UO_2(CO_3)_3$, which has neutral valence. At this pH, adsorption is likely influenced by electrostatic interactions. However, the marginally lower adsorption in $MgCl_2$ suggests that magnesium may exhibit a unique non-affinity for uranium adsorption. Additionally, the similar adsorption capacity of $Ca_2UO_2(CO_3)_3$ compared to other charged uranyl complexes suggests the presence of unidentified adsorption mechanisms. Since the adsorbed uranium is of a very low weight percentage relative to the membrane, it may be classified as low-level waste under the Nuclear Regulatory Commission, which oversees the management of radioactive materials.[13]

Membrane selectivity

We investigated the membrane selectivity (MS) of NF90 and NF270 membranes, focusing on their capability to differentiate between uranium(VI) ions and common cations (Na^+, Mg^{2+}, Ca^{2+}) in solution. MS is a dimensionless value representing the transmission ratio of one ion relative to another through a membrane under identical conditions. This study's higher MS value establishes that the membrane is selectively more permeable to selected cations than uranium. The objective was to evaluate the effect of pH change on each membrane's selectivity response, and Fig. 5 illustrates the selectivity responses of NF90 and NF270 throughout a pH range of 4–10. The experimental setup kept a constant uranium(VI) concentration (150 μg L^{-1}) while varying the concentrations of Na^+, Mg^{2+}, and Ca^{2+} to assess their individual selectivity against uranium(VI), calculated using eqn (3).

The results show similar trends for both membranes: the MS is higher at neutral pH and decreases at pH extremes, with a slightly higher MS observed in basic conditions than in acidic ones. NF90 exhibited a more pronounced difference in MS than NF270, possibly due to NF90's higher ion rejection rates. The difference in MS between the monovalent sodium ions and the divalent magnesium and calcium ions showed monovalent ions had a larger calculated MS, by approximately an order of magnitude (from ~200 to ~10, respectively, at pH 7) for NF90. For NF270, the difference between mono- and divalent ions is less pronounced. Typically, increasing cation concentrations resulted in decreased MS values for the NF90. The governing mechanism for MS appears to involve a combination of steric hindrance and charge interactions, as suggested by Zhang *et al.*[55] Our data supports this hypothesis, with monovalent sodium ion showing higher MS values and the heavier divalent calcium ion typically displaying lower MS values than divalent magnesium ion. MS results demonstrate that both membranes are effective and precise in separating ions in feed water that are similar to natural groundwater.

Conclusion

This study investigated uranium removal from groundwater capabilities of two commercially available nanofiltration membranes, NF90 and NF270. Both membranes were systematically evaluated across various naturally relevant pH conditions and cations found in groundwater. Our findings show that the NF90 can produce permeate that meets EPA drinking water limits regarding uranium (<30 μg L). The NF270 also effectively removed uranium, but due to the sensitivity to Donnan exclusion mechanisms, a reduced performance was observed, as such the EPA drinking water standard at pH 4 was not met for all solutions studied. Uranium adsorption was observed in both membranes and occurs in greater capacity at a neutral pH than at low pH. The quantity of uranium adsorbed to the polyamide layer does not seem to be at a level that would create disposal issues with radioactive waste regulations. The membrane selectivity experiments also showcased both membranes' ability to selectively remove ions, which can ultimately be used for potable water without the need for remineralization of the product water. Insights gained from this work further our understanding of nanofiltration membranes for water treatment and in mitigating uranium contamination from groundwater.

Open Access Article. Published on 25 Fõndo 2024. Downloaded on 13/2/2026 19:33:08.
This article is licensed under a Creative Commons Attribution 3.0 Unported Licence.

Implications

Access to clean water is an essential human right, and the implications of this study extend beyond technical solutions, addressing a problem that affects many populations worldwide. The efficacy of NF in removing uranium, shown by this study, opens the possibility of addressing health risks to those exposed to uranium in their drinking water. There is extensive literature on the cost-effectiveness of NF water treatment as a viable solution in resource-constrained locations, and this study also shows viability in using environmentally relevant ionic concentrations while using operational conditions (such as feed water pressure) which mimic a low energy demand system. Further studies are needed to consider temperature gradients that would occur in a pilot scale setting, which this study did not attempt.

Data availability

Data for this article, including experimental logs are available at University of Arizona repository and stored in laboratory google drives in excel format.

The data supporting this article have been included as part of the ESI.†

Conflicts of interest

There are no conflicts to declare.

Acknowledgements

We would like to acknowledge the National Science Foundation provided PhD studentship funding *via*: NRT-INFEWS: Indigenous Food, Energy, and Water Security and Sovereignty (IndigeFEWSS) Award Number DGE #1735173. Additionally, we would like to thank the Sloan Foundation and the University of Arizona Agnes Nelms Haury Foundation that provided funding for student support and for lab materials to conduct this research.

References

1 UN, *Summary Progress Update 2021: SDG 6 — water and sanitation for all. UN-Water integrated monitoring initiative*, 2021.

2 T. Gleeson, M. Cuthbert, G. Ferguson and D. Perrone, Global Groundwater Sustainability, Resources, and Systems in the Anthropocene, *Annu. Rev. Earth Planet. Sci.*, 2020, **48**(1), 431–463, DOI: **10.1146/annurev-earth-071719-055251**.

3 J. Rajapakse, B. Hudson and C. Brown, *Poor Water Quality and Related Health Issues in Remote Indigenous Populations of Some of the World's Wealthiest Nations*, 2022.

4 J. Hoover, M. Gonzales, C. Shuey, Y. Barney and J. Lewis, Elevated Arsenic and Uranium Concentrations in Unregulated Water Sources on the Navajo Nation, USA, *Exposure Health*, 2017, **9**(2), 113, Available from: **https://www.ncbi.nlm.nih.gov/pubmed/28553666**.

5 J. C. Ingram, L. Jones, J. Credo and T. Rock, Uranium and arsenic unregulated water issues on Navajo lands, *J. Vac. Sci. Technol., A*, 2020, **38**(3), 31003, DOI: **10.1116/1.5142283**.

6 L. Newsome, K. Morris and J. R. Lloyd, The biogeochemistry and bioremediation of uranium and other priority radionuclides, *Chem. Geol.*, 2014, **363**, 164–184.

7 B. Liu, T. Peng, H. Sun and H. Yue, Release behavior of uranium in uranium mill tailings under environmental conditions, *J. Environ. Radioact.*, 2017, **171**, 160–168, DOI: **10.1016/j.jenvrad.2017.02.016**.

8 M. L. Zamora, B. L. Tracy, J. M. Zielinski, D. P. Meyerhof and M. A. Moss, Chronic Ingestion of Uranium in Drinking Water: A Study of Kidney Bioeffects in Humans, *Toxicol. Sci.*, 1998, **43**(1), 68–77, DOI: **10.1006/toxs.1998.2426**.

9 A. Younes, J. S. Ali, A. Duda, C. Alliot, S. Huclier-Markai and J. Wang, *et al.*, Uptake and Removal of Uranium by and from Human Teeth, *Chem. Res. Toxicol.*, 2021, **34**(3), 880–891, DOI: **10.1021/acs.chemrestox.0c00503**.

10 L. Jones, J. Credo, R. Parnell and J. C. Ingram, Dissolved Uranium and Arsenic in Unregulated Groundwater Sources – Western Navajo Nation, *J. Contemp. Water Res. Educ.*, 2020, **169**(1), 27–43, DOI: **10.1111/j.1936-704X.2020.03330.x**.

11 G. Bernhard, G. Geipel, V. Brendler and H. Nitsche, Uranium speciation in waters of different uranium mining areas, *J. Alloys Compd.*, 1998, **271–273**, 201–205.

12 L. A. Richards, B. S. Richards and A. I. Schäfer, Renewable energy powered membrane technology: Salt and inorganic contaminant removal by nanofiltration/reverse osmosis, *J. Membr. Sci.*, 2011, **369**(1), 188–195, DOI: **10.1016/j.memsci.2010.11.069**.

13 U.S. EPA, *A Regulators' Guide to the Management of Radioactive Residuals from Drinking Water Treatment Technologies*, 2005, [cited 2024 Mar 17]. Available from: https://www.epa.gov/radiation/tenorm-drinking-water-treatment-residuals.

14 P. D. Bhalara, D. Punetha and K. Balasubramanian, A review of potential remediation techniques for uranium(VI) ion retrieval from contaminated aqueous environment, *J. Environ. Chem. Eng.*, 2014, **2**(3), 1621–1634, DOI: **10.1016/j.jece.2014.06.007**.

15 A. W. Mohammad, Y. H. Teow, W. L. Ang, Y. T. Chung, D. L. Oatley-Radcliffe and N. Hilal, Nanofiltration membranes review: Recent advances and future prospects, *Desalination*, 2015, **356**, 226–254, DOI: **10.1016/j.desal.2014.10.043**.

16 A. Favre-Reguillon, G. Lebuzit, J. Foos, A. Guy, M. Draye and M. Lemaire, Selective Concentration of Uranium from Seawater by Nanofiltration, *Ind. Eng. Chem. Res.*, 2003, **42**(23), 5900–5904.

17 Y. Chung, Y. M. Yun, Y. J. Kim, Y. S. Hwang and S. Kang, Preparation of alumina-zirconia (Al-Zr) ceramic nanofiltration (NF) membrane for the removal of uranium in aquatic system, *Water Sci. Technol.: Water Supply*, 2019, **19**(3), 789–795.

18 C. Xing, B. Bernicot, G. Arrachart and S. Pellet-Rostaing, Application of ultra/nano filtration membrane in uranium rejection from fresh and salt waters, *Sep. Purif. Technol.*, 2023, **314**, 123543.

 This journal is © The Royal Society of Chemistry 2024

Open Access Article. Published on 25 Föndo 2024. Downloaded on 13/2/2026 19:33:08. This article is licensed under a Creative Commons Attribution 3.0 Unported Licence.

19 R. Lamsal, S. G. Harroun, C. L. Brosseau and G. A. Gagnon, Use of surface enhanced Raman spectroscopy for studying fouling on nanofiltration membrane, *Sep. Purif. Technol.*, 2012, **96**, 7–11, Available from: **http://www.sciencedirect.com/science/article/pii/S1383586612002912**.

20 E. Steinle-Darling and M. Reinhard, Nanofiltration for Trace Organic Contaminant Removal: Structure, Solution, and Membrane Fouling Effects on the Rejection of Perfluorochemicals, *Environ. Sci. Technol.*, 2008, **42**(14), 5292–5297.

21 J. V. Nicolini, C. P. Borges and H. C. Ferraz, Selective rejection of ions and correlation with surface properties of nanofiltration membranes, *Sep. Purif. Technol.*, 2016, **171**, 238–247.

22 O. Raff and R. D. Wilken, Removal of dissolved uranium by nanofiltration, *Desalination*, 1999, **122**(2), 147–150, Available from: **https://www.sciencedirect.com/science/article/pii/S0011916499000351**.

23 A. Favre-Réguillon, G. Lebuzit, D. Murat, J. Foos, C. Mansour and M. Draye, Selective removal of dissolved uranium in drinking water by nanofiltration, *Water Res.*, 2008, **42**(4–5), 1160–1166, Available from: **https://linkinghub.elsevier.com/retrieve/pii/S0043135407005775**.

24 M. G. Torkabad, A. R. Keshtkar and S. J. Safdari, Comparison of polyethersulfone and polyamide nanofiltration membranes for uranium removal from aqueous solution, *Prog. Nucl. Energy*, 2017, **94**, 93–100, DOI: **10.1016/j.pnucene.2016.10.005**.

25 E. E. M. Oliveira, C. C. R. Barbosa and J. C. Afonso, Selectivity and structural integrity of a nanofiltration membrane for treatment of liquid waste containing uranium, *Membr. Water Treat.*, 2012, **3**(4), 231–242.

26 H. M. A. Schulte-Herbruggen, Remote Community Drinking Water Supply – Mechanisms of Uranium Retention and Adsorption by Ultrafiltration, Nanofiltration and Reverse Osmosis, *Dissertation*, The University of Edinburgh, Edinburgh, 2011, p. 257.

27 J. Schaep, B. Van der Bruggen, C. Vandecasteele and D. Wilms, Influence of ion size and charge in nanofiltration, *Sep. Purif. Technol.*, 1998, **14**(1–3), 155–162, DOI: **10.1016/s1383-5866(98)00070-7**.

28 W. Cheng, C. Liu, T. Tong, R. Epsztein, M. Sun and R. Verduzco, *et al.*, Selective removal of divalent cations by polyelectrolyte multilayer nanofiltration membrane: Role of polyelectrolyte charge, ion size, and ionic strength, *J. Membr. Sci.*, 2018, **559**, 98–106, Available from: **https://linkinghub.elsevier.com/retrieve/pii/S0376738818301947**.

29 R. Epsztein, E. Shaulsky, N. Dizge, D. M. Warsinger and M. Elimelech, Role of Ionic Charge Density in Donnan Exclusion of Monovalent Anions by Nanofiltration, *Environ. Sci. Technol.*, 2018, **52**(7), 4108–4116, DOI: **10.1021/acs.est.7b06400**.

30 M. Hoyer, D. Zabelt, R. Steudtner, V. Brendler, R. Haseneder and J. U. Repke, Influence of speciation during membrane treatment of uranium contaminated water, *Sep. Purif. Technol.*, 2014, **132**, 413–421, DOI: **10.1016/j.seppur.2014.05.044**.

31 P. L. Smedley and D. G. Kinniburgh, Uranium in natural waters and the environment: Distribution, speciation and impact, *Appl. Geochem.*, 2023, **148**, 105534.

32 M. S. Alam and T. Cheng, Uranium release from sediment to groundwater: Influence of water chemistry and insights into release mechanisms, *J. Contam. Hydrol.*, 2014, **164**, 72–87, DOI: **10.1016/j.jconhyd.2014.06.001**.

33 P. M. Fox, J. A. Davis and J. M. Zachara, The effect of calcium on aqueous uranium(VI) speciation and adsorption to ferrihydrite and quartz, *Geochim. Cosmochim. Acta*, 2006, **70**(6), 1379–1387.

34 J. P. Gustafsson, *Visual MINTEQ*, 2013.

35 O. Peer-Haim, I. Shefer, P. Singh, O. Nir and R. Epsztein, The Adverse Effect of Concentration Polarization on Ion-Ion Selectivity in Nanofiltration, *Environ. Sci. Technol. Lett.*, 2023, **10**(4), 363–371, DOI: **10.1021/acs.estlett.3c00124**.

36 A. W. Mohammad, Simple mass transfer experiment using nanofiltration membranes, *Chem. Eng. Educ.*, 2000, **34**(3), 264–267.

37 I. Sutzkover, D. Hasson and R. Semiat, Simple technique for measuring the concentration polarization level in a reverse osmosis system, *Desalination*, 2000, **131**(1–3), 117–127.

38 A. E. Childress and M. Elimelech, Effect of solution chemistry on the surface charge of polymeric reverse osmosis and nanofiltration membranes, *J. Membr. Sci.*, 1996, **119**(2), 253–268, Available from: **https://linkinghub.elsevier.com/retrieve/pii/0376738896001275**.

39 L. D. Nghiem, A. I. Schäfer and M. Elimelech, Removal of Natural Hormones by Nanofiltration Membranes: Measurement, Modeling, and Mechanisms, *Environ. Sci. Technol.*, 2004, **38**(6), 1888–1896, DOI: **10.1021/es034952r**.

40 C. Y. Tang, Y. N. Kwon and J. O. Leckie, Effect of membrane chemistry and coating layer on physiochemical properties of thin film composite polyamide RO and NF membranes, *Desalination*, 2009, **242**(1–3), 149–167, Available from: **https://linkinghub.elsevier.com/retrieve/pii/S0011916409002215**.

41 C. E. Harvie, N. Møller and J. H. Weare, The prediction of mineral solubilities in natural waters: The Na-K-Mg-Ca-H-Cl-SO4-OH-HCO3-CO3-CO2-H2O system to high ionic strengths at 25°C, *Geochim. Cosmochim. Acta*, 1984, **48**(4), 723–751, Available from: **https://linkinghub.elsevier.com/retrieve/pii/001670378490098X**.

42 J. Zhao, I. I. Fasfous, J. D. Murimboh, T. Yapici, P. Chakraborty and S. Boca, *et al.*, Kinetic study of uranium speciation in model solutions and in natural waters using Competitive Ligand Exchange Method, *Talanta*, 2009, **77**(3), 1015–1020, DOI: **10.1016/j.talanta.2008.07.057**.

43 A. M. Giblin, B. D. Batts and D. J. Swaine, Laboratory simulation studies of uranium mobility in natural waters, *Geochim. Cosmochim. Acta*, 1981, **45**(5), 699–709.

44 C. Götz, G. Geipel and G. Bernhard, The influence of the temperature on the carbonate complexation of uranium(VI): a spectroscopic study, *J. Radioanal. Nucl. Chem.*, 2010, **287**(3), 961–969, Available from: **https://akjournals.com/view/journals/10967/287/3/article-p961.xml**.

Open Access Article. Published on 25 Föndo 2024. Downloaded on 13/2/2026 19:33:08.
This article is licensed under a Creative Commons Attribution 3.0 Unported Licence.

45 C. Fillaux, D. Guillaumont, J. C. Berthet, R. Copping, D. K. Shuh and T. Tyliszczak, *et al.*, Investigating the electronic structure and bonding in uranyl compounds by combining NEXAFS spectroscopy and quantum chemistry, *Phys. Chem. Chem. Phys.*, 2010, **12**(42), 14253–14262.

46 E. S. Stoyanov, V. A. Mikhailov, V. G. Torgov and T. V. Us, Structure and composition of the polymeric products of UO2SO4 extraction by benzene solutions of uranyl bis(2-ethylhexyl) phosphate, *J. Struct. Chem.*, 1995, **36**(4), 619–625, DOI: **10.1007/BF02578653**.

47 K. Gückel, S. Tsushima and H. Foerstendorf, Structural characterization of the aqueous dimeric uranium(vi) species: (UO2)2CO3(OH)3−, *Dalton Trans.*, 2013, **42**(28), 10172–10178.

48 S. D. Kelly, K. M. Kemner and S. C. Brooks, X-ray absorption spectroscopy identifies calcium-uranyl-carbonate complexes at environmental concentrations, *Geochim. Cosmochim. Acta*, 2007, **71**(4), 821–834.

49 B. D. Stewart, M. A. Mayes and S. Fendorf, Impact of Uranyl–Calcium–Carbonato Complexes on Uranium(VI) Adsorption to Synthetic and Natural Sediments, *Environ. Sci. Technol.*, 2010, **44**(3), 928–934, DOI: **10.1021/es902194x**.

50 P. Robinson, *Uranium Mill Tailings Remediation Performed by the US DOE: An Overview*, Albuquerque, 2004, May.

51 A. Abdelouas, W. Lutze and E. Nuttall, Chemical reactions of uranium in ground water at a mill tailings site, *J. Contam. Hydrol.*, 1998, **34**(4), 343–361, DOI: **10.1016/S0169-7722(98)00097-7**.

52 Y. Kitano and T. Oomori, The coprecipitation of uranium with calcium carbonate, *J. Oceanogr. Soc. Jpn.*, 1971, **27**(1), 34–42, DOI: **10.1007/BF02109313**.

53 K. Boussu, Y. Zhang, J. Cocquyt, P. Van der Meeren, A. Volodin and C. Van Haesendonck, *et al.*, Characterization of polymeric nanofiltration membranes for systematic analysis of membrane performance, *J. Membr. Sci.*, 2006, **278**(1), 418–427, Available from: **http://www.sciencedirect.com/science/article/pii/S0376738805008367**.

54 A. Escoda, P. Fievet, S. Lakard, A. Szymczyk and S. Déon, Influence of salts on the rejection of polyethyleneglycol by an NF organic membrane: Pore swelling and salting-out effects, *J. Membr. Sci.*, 2010, **347**(1–2), 174–182.

55 H. Zhang, Q. He, J. Luo, Y. Wan and S. B. Darling, Sharpening Nanofiltration: Strategies for Enhanced Membrane Selectivity, *ACS Appl. Mater. Interfaces*, 2020, **12**(36), 39948–39966, DOI: **10.1021/acsami.0c11136**.

 This journal is © The Royal Society of Chemistry 2024